FULL-SCALE SHAKE TABLE INVESTIGATION OF BRIDGE ABUTMENT LATERAL EARTH PRESSURE

Patrick Wilson[1] and Ahmed Elgamal[2]

SUMMARY

During strong seismic excitation, passive earth pressure at the abutments may provide resistance to longitudinal displacement of the bridge deck. The dynamic pressure component may also contribute to undesirable abutment movement or damage. Current uncertainty in the passive force-displacement relationship and in the dynamic response of abutment backfills continues to motivate large-scale experimentation. In this regard, a test series is conducted to measure static and dynamic lateral earth pressure on a 1.7 meter high bridge abutment wall. Built in a large soil container, the wall is displaced horizontally into the dense sand backfill, in order to record the passive force-displacement relationship. The wall-backfill system is also subjected to shake table excitation. In the conducted tests, lateral earth pressure on the wall remained close to the static value during the low to moderate shaking events (up to about 0.5g). At higher levels of input acceleration, a substantial portion of the backfill inertial force started to clearly act on the wall.

INTRODUCTION

A collaborative effort has been underway to further study the behaviour of reinforced concrete highway bridges during earthquakes [1]. For that purpose, facilities of the George E. Brown, Jr. Network for Earthquake Engineering Simulation (NEES, http://nees.org) have been utilized to conduct large-scale experiments at the University of Nevada, Reno (UNR) and the University of California, San Diego (UCSD). The focus of this discussion is a series of abutment-backfill interaction tests [2], conducted at the NEES UCSD Large High Performance Outdoor Shake Table (LHPOST).

Abutment-bridge interaction remains a topic of current research interest [2-7]. For instance, a new dynamic active earth pressure approach by Koseki et al. [8] has been validated recently [9], and adopted for seismic bridge design in Japan [7]. Damage resulting from this type of interaction was reported at several bridges after the 1995 Hyogo-Ken Nanbu Kobe earthquake [7].

In the U.S. practice [10-12], a seat abutment with a sacrificial backwall is suggested (Figure 1). This design approach aims to protect the abutment foundation, by allowing the backwall to become sheared-off, if impacted by the bridge deck. As such, the force-displacement relationship at the abutment is primarily dictated by the backfill passive earth resistance [3]. Current estimates of this abutment lateral stiffness and capacity [11] are based on limited data from static passive earth pressure tests [13], and recent research continues to provide new insights [2-6].

In addition to the static capacity, inertial effects on the abutment and backfill may influence the actual available resistance (Figure 1). Based on the fundamental work of Mononobe and Matsuo [14] and Okabe [15], Kramer [16] shows that dynamic excitation may cause the instantaneous passive resistance to be lower than that of the corresponding static case.

In order to address the above considerations, a series of experiments was conducted to measure static and dynamic earth pressure on a bridge abutment backwall (Figure 1). First, a passive earth pressure force-displacement relationship was recorded by pushing the backwall into the static dense sand backfill. Next, dynamic response caused by shake table excitation was measured in the form of wall forces and backfill accelerations. Dynamic tests were conducted near the at-rest and the passive earth pressure conditions. In this fashion, the recorded dynamic data would be of relevance to: i) the backwall-bridge interaction scenarios described above, and ii) assessments of seismic forces on non-yielding-type retaining structures. In the following sections, the tests are described and the results are presented and discussed.

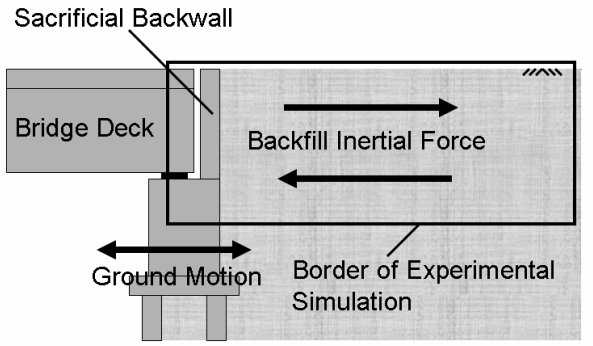

Figure 1: ***Schematic bridge abutment elevation view showing backfill inertial force.***

[1] *Graduate Student Researcher, Department of Structural Engineering, University of California San Diego, La Jolla, CA 92093-0085 USA prwilson@ucsd.edu*

[2] *Professor, Department of Structural Engineering, University of California San Diego, La Jolla, CA 92093-0085 USA elgamal@ucsd.edu*

EXPERIMENTAL INVESTIGATION

Test Facility

In April of 2005, UCSD officially opened the Englekirk Structural Engineering Center (ESEC). For seismic applications, this outdoor facility consists of 2 large in-ground soil pits and a shake table. Experiments for the presented study were performed on the 12.2 m (40 ft) by 7.6 m (25 ft) outdoor shake table (Figure 2). Funded by NEES (http://nees.ucsd.edu), the shake table is currently capable of supporting a vertical payload of 20 MN [17, 18], and producing uniaxial motions of up to 3g (acceleration), 1.8 m/s (velocity) and 0.75 m (displacement). The lateral earth pressure experiments described in this paper (Figure 2) are the first soil-structure interaction tests performed on this new outdoor shake table [2].

Figure 2: Soil model container on the NEES outdoor shake table at UCSD.

Experimental Configuration

An available laminar soil container, restrained to perform as a rigid box (Figure 2), was employed for the earth pressure experiments. The inside dimensions of the container were 6.71 m (22') long by 2.90 m (9'6") wide by 2.54 m (8'4") tall in this experimental setup. Additional frames are available for creating a taller configuration (up to 5 m in height). Between the backfill and the sides of the container, friction was reduced (on the order of 2% of the measured peak passive load [2]) by employing a three layer smooth, thin plastic-liner system (Figure 3c).

The test wall was constructed of reinforced concrete, with dimensions of 0.2 m in thickness, 2.74 m in width and 2.13 m in height (Figure 3c). The wall was suspended by a steel beam which moves freely along the upper track of the container (Figure 3a, b and c). In this suspended configuration, the wall was unconstrained from lateral motion along its horizontal and vertical boundaries. The combined mass of the wall and supporting beam was 4500 kg.

Behind the wall, four jack and load cell stacks (Figure 3d) reacted on concrete filled steel-shell posts. These jacks were used to push the wall into the backfill in order to record the static passive force-displacement relationship. A manifold system allowed for distribution of pressure to the four jacks from a single pump. Flow to each jack was controlled individually to help maintain a vertical orientation as the wall translated into the backfill. Closing the valves to all 4 jacks locked the wall at any desired level of displacement.

Backfill

The backfill was 5.6 m long (L), 2.87 m wide and 2.14 m tall. A 1.7 m height (H) backfill (5.5' as a typical bridge backwall height [3]) was supported by the test wall, with the remainder of the backfill extending below (Figure 3c). Well-graded sand

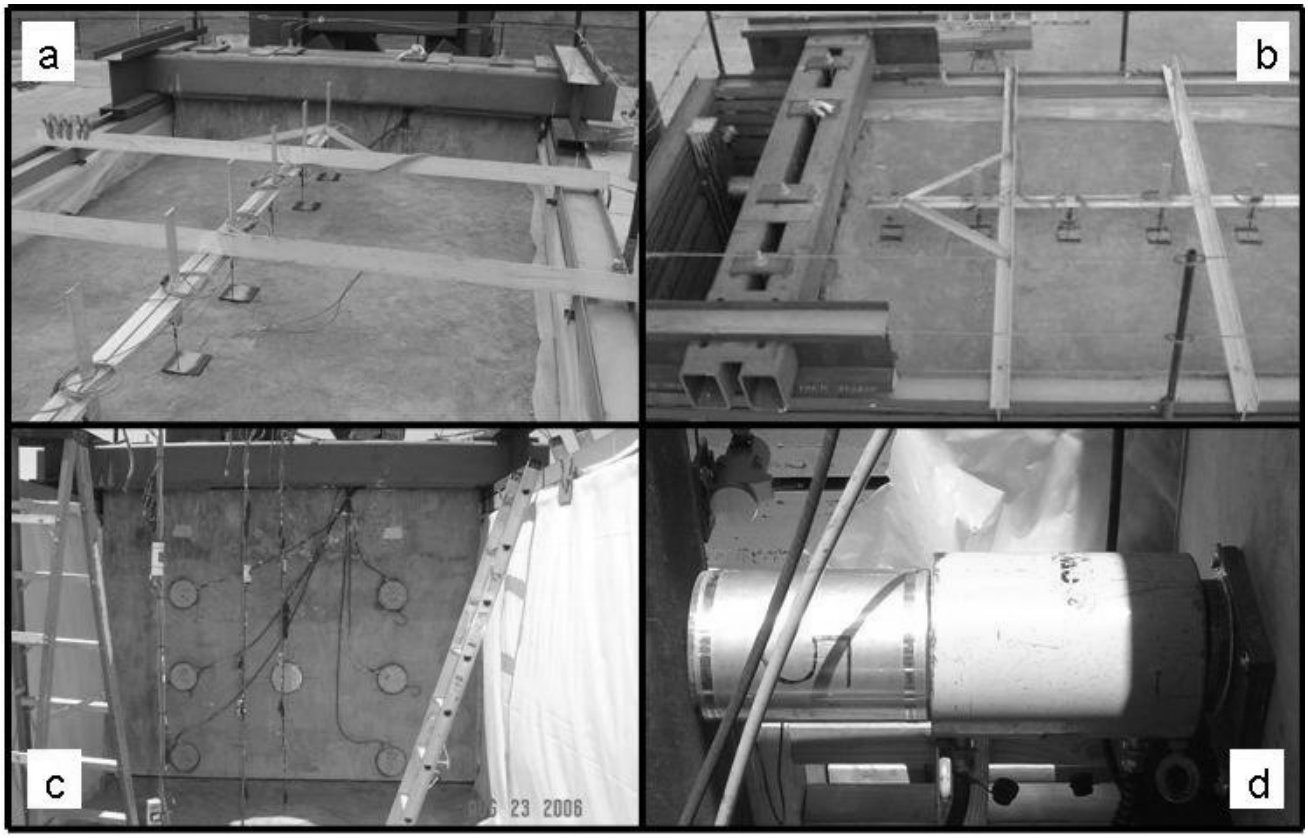

Figure 3: Experimental configuration photographs; a) Backfill surface, b) Elevated side view, c) Wall inside container before backfilling, d) Load cell (left) and jack (right) behind wall.

(with 7% fines) was placed in small lifts and compacted in compliance with Caltrans [19] structural backfill requirements. Compaction of each lift reached at least 95% (according to nuclear gauge measurements) of the density achieved in ASTM Standard Method D1557 tests (95% relative compaction). Table 1 summarizes additional characteristics of the backfill material in its compacted state.

Table 1. Compacted backfill characteristics.

USCS (Unified Soil Classification System)	Well graded sand / silty sand
Gravel content	1%
Sand content	92%
Fines content	7%
Approximate water content at placement	8.50%
Moist unit weight	20.6 kN/m^3
Plane-strain friction angle Φ [a,b]	50 degrees
Cohesion intercept c [c]	14 kN/m^2

[a] Determined from analysis of the static passive pressure test

[b] Corresponding to a Φ = 42 degrees in a triaxial test [27]

[c] Determined from direct shear testing [2]

Instrumentation

As mentioned above, 4 load cells were installed behind the wall (Figure 3d) to measure the lateral compressive forces. As such, the load cell readings during dynamic testing were due to the combined inertial forces of the backfill and the wall.

String potentiometers measured displacement of the wall into the backfill. Linear potentiometers measured vertical displacement of the wall and vertical heave or settlement of the backfill (shown mounted on an aluminium frame in Figs. 3a and 3b). A total of 42 accelerometers located inside the backfill and at various locations on the soil box were added to the model before the start of dynamic testing (Fig. 3c).

Passive Earth Pressure Test on Static Backfill

Passive earth resistance due to displacement of the abutment backwall was measured first. The hydraulic jacks pushed the wall into the backfill up to and beyond peak load (the backbone curve is shown in Figure 4). Measurement of this conservative (lower-bound) passive earth resistance was achieved by permitting the backwall to move vertically along with the adjacent backfill soil [2], thus limiting the development of wall-soil friction (2.6 degrees in this test [2, 20]).

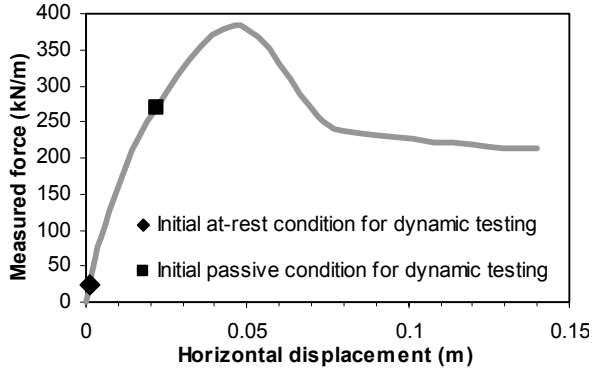

Figure 4: ***Backbone load-deflection curve (normalized per meter of abutment width) from results of test on static backfill.***

As shown in Figure 4, the wall experienced a peak passive resistance of 385 kN/m (normalized per meter of wall width) at a horizontal displacement of 0.046 m (2.7% of the wall height). Thereafter, softening behaviour of the densely compacted sand backfill occurred [21, 22], eventually leading to a residual resistance of 212 kN/m (about 55% of the peak value).

Observations based on results from this passive static earth pressure test include [2]:

1. The measured peak passive resistance closely agrees with the Log-Spiral Theory estimate [21].
2. The Caltrans [11] and AASHTO [12] abutment load-deflection models agree fairly well with the experimentally measured counterparts, both in stiffness and peak resistance levels.
3. The above models [11, 12] do not represent the observed large strain softening behaviour (Figure 4). Consequently, at displacements beyond 0.05 m (Figure 4), these models become increasingly non-conservative compared to the test results.

Dynamic Lateral Earth Pressure Tests

Dynamic lateral forces were first measured during a series of shake table input motions with the abutment wall starting from a near at-rest condition (Figure 4). Next, the wall was pushed statically into the backfill, mobilizing 2/3 of the peak passive resistance approximately (Figure 4). A second series of shake table tests was then conducted in this new passive pressure configuration. In these dynamic excitation tests, the hydraulic jacks (Figure 3d) were locked in a fixed position to essentially shake the wall and backfill with the same motion. As with the case of the static passive pressure test, all force measurements presented below will be reported per meter of wall width.

Input motion and system performance

A modified acceleration time history from the Century City Station record of the 1994 Northridge, California earthquake was developed for use in this NEES collaborative highway bridge investigation [1]. The baseline Shake Table Motion (STM) was a scaled version with peak acceleration of about 0.4g approximately. The shaking was 1-dimensional in the direction of the normal to the wall face.

Natural frequencies of the wall-soil system were identified at about 13 Hz and above. As a representative of strong ground motion excitation, the STM was of significantly lower frequency content. At these lower frequencies, the backfill responded generally in phase with the base acceleration (Figure 5) with only minor amplification and phase difference effects [2, 23].

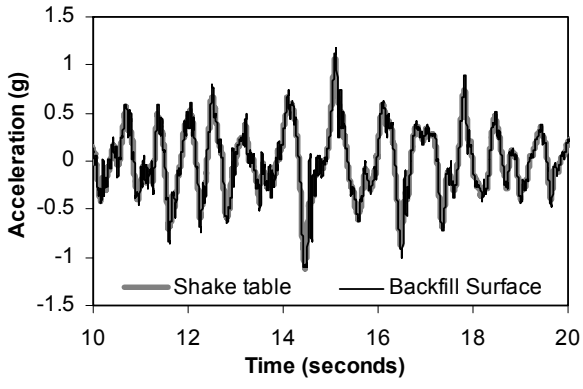

Figure 5: ***Representative shake table acceleration and backfill response near top of wall.***

At-Rest Condition Dynamic Tests

Following the static passive earth pressure test described above, the backfill was removed and an array of accelerometers was installed throughout the soil container (Figure 3c). After soil placement and compaction, the wall was pushed slightly (about 2.5 mm) toward the backfill in order to ensure that all four load cells (Figure 3d) were registering a small reading. With the wall in this position, the valve to each jack was closed to provide this near at-rest initial earth pressure condition (Figure 4).

Next, input excitations of 100%, 200%, and 300% (1x, 2x, and 3x) of the STM were imparted by the shake-table. Figures 6 through 8 show the total force measured by the load cells, and the acceleration response near the wall at the backfill surface (shown in Figure 5 to be similar to the base acceleration) during these tests.

In Figure 6, with peak acceleration of about 0.4g (1x STM), the measured thrust remained within plus or minus 5 kN/m of the 26 kN/m at-rest force on the wall. Doubling and tripling the input STM (Figures 7 and 8) resulted in measured dynamic thrusts that approached 3 and 14 times those of Figure 6, respectively. During the strongest shaking event, the measured load was seen to reach zero at some instances (Figure 8), as the inertial forces fully relieved the statically imposed lateral stress.

Logically, dynamic earth pressure is conventionally correlated with lateral acceleration [8, 9, 14-16, 24-26]. Such a relationship is illustrated in Figure 9, which directly compares

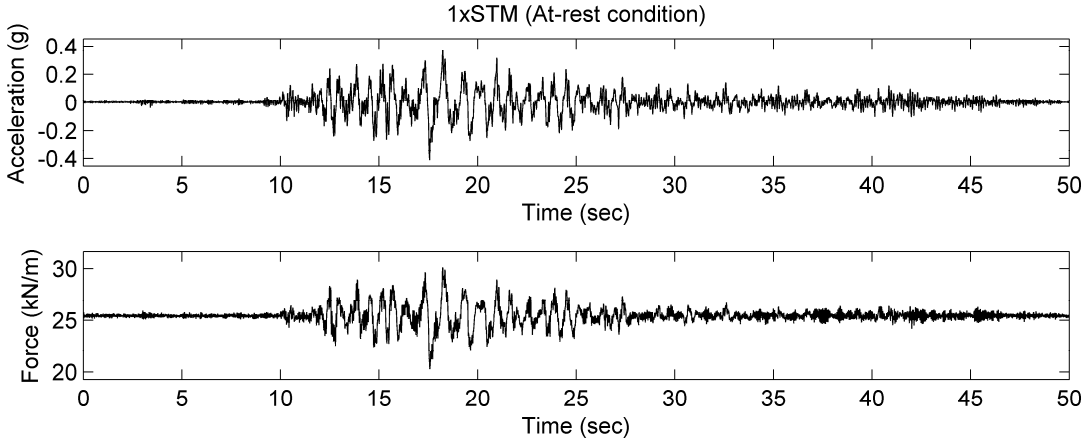

Figure 6: ***Backfill response acceleration and total load cell force for the baseline STM event (near at-rest condition).***

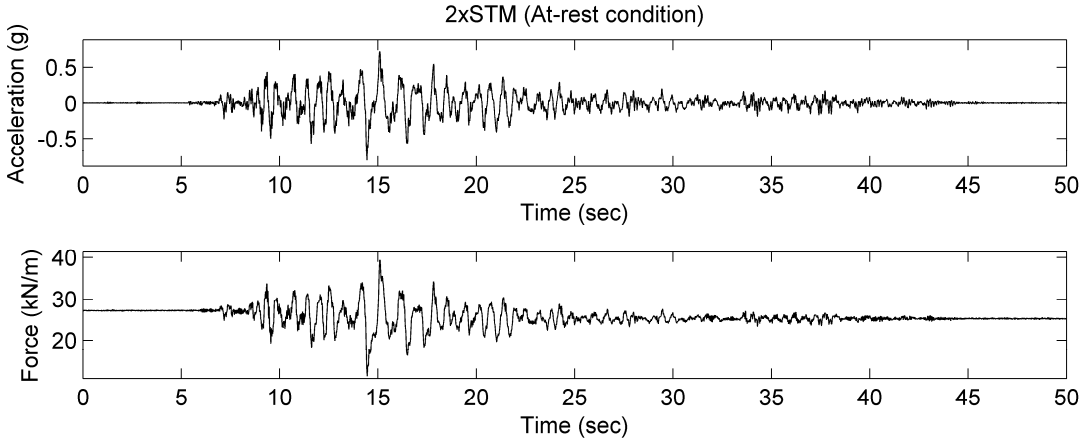

Figure 7: ***Backfill response acceleration and total load cell force for 2 x STM (near at-rest condition).***

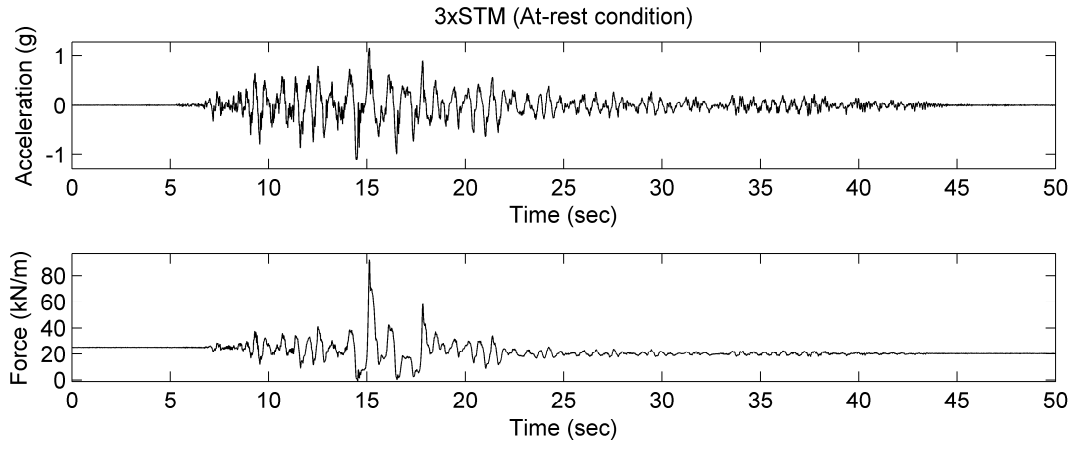

Figure 8: ***Backfill response acceleration and total load cell force for 3 x STM (near at-rest condition).***

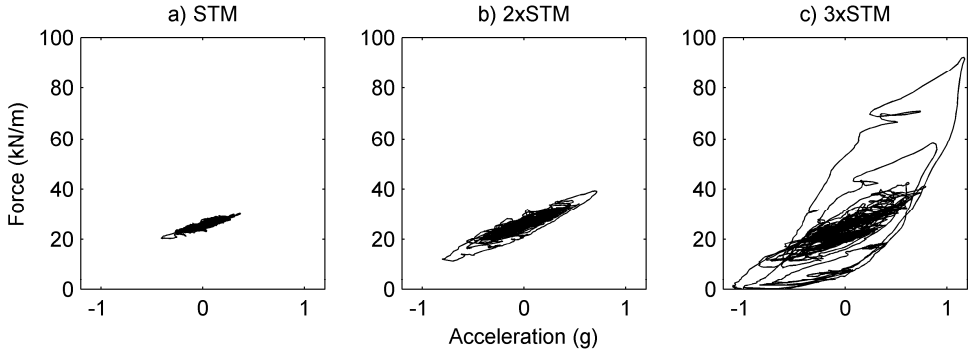

Figure 9: ***Total load cell force versus backfill acceleration (near at-rest condition).***

the force measured by the load cells behind the wall (Figure 3d) with the backfill response acceleration. For the lower level shaking STM test (Figure 9a), the relationship between the measured force and acceleration followed a relatively linear pattern. When stronger shaking took place (Figure 9c) there was a sharp increase in the rate at which the force changed relative to the backfill acceleration (starting around 0.5g). To verify this strong shaking trend, an even stronger excitation (330% or 3.3xSTM) was also performed, and a similar trend in the force-acceleration relationship (not shown) was observed [2].

Analysis of the Experimental Observations

Measured by the load cells behind the wall (Figure 3d), the force of Figures 6 through 9 includes the wall inertia along with the static and dynamic lateral earth pressure. Upon contact, a bridge deck would experience this force. At the instants of peak thrust, Figure 10 displays the relationship between the dynamic component of these forces and the backfill acceleration.

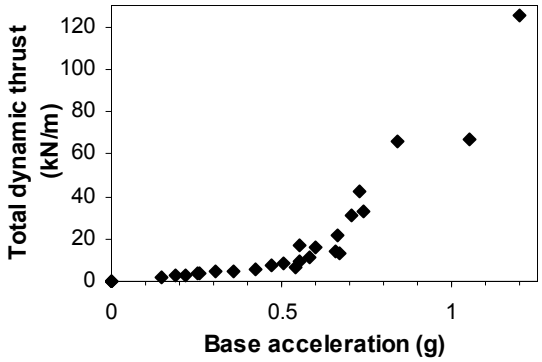

Figure 10: ***Total dynamic thrust (including wall inertia) during 3xSTM and 3.3xSTM tests.***

In order to examine the dynamic earth pressure component separately, Figure 11 displays the thrust after removal of the wall inertial force from the values of Figure 10. At accelerations above the level of above 0.5g, significant backfill inertial forces clearly begin to act on the wall (Figure 11). Below this level of acceleration, relatively minor changes in earth pressure were observed (Figure 11).

During earlier experiments conducted by Nakamura [27] and Sitar and Al Atik [28], it was likewise observed that the dynamic earth pressure increment was small for shaking at comparable low levels. In addition, a similar pattern of response is depicted in Figure 12, where cohesion was included in a M-O [14, 15] type approach [29]. The normalized quantity (C/γH, Figure 12) for our test wall is about 0.3, corresponding to the curve furthest to the right with a zero earth pressure increment up to slightly more than 0.5g. This effect of cohesion on dynamic earth pressure (Figure 12) agrees well with the experimental trends of Figure 11. As such, the added shear strength provided by cohesion (Table 1) in the backfill (resulting from heavy compaction and the 7 percent fines mentioned above) appears to be a primary reason for the dynamic earth pressure increment to be quite small in the experiments up to about 0.5g of shaking. In other words, the small amount of fines in the backfill material (Table 1) may be considered as beneficial for reducing the dynamic earth pressure on the wall.

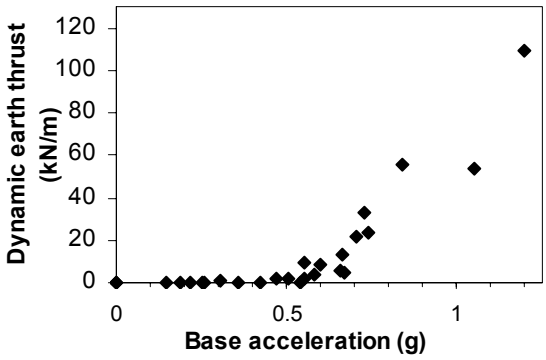

Figure 11: ***Dynamic earth thrust (wall inertia removed) during 3xSTM and 3.3xSTM tests.***

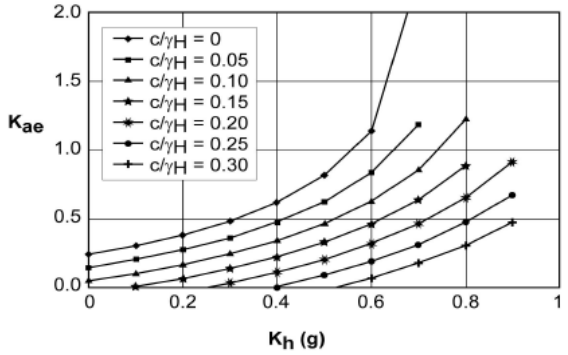

Figure 12: ***Estimated earth pressure coefficient based on Mononobe-Okabe equations with added cohesion (from Anderson et al. [29]).***

Passive Pressure Condition Dynamic Tests

Following the at-rest condition dynamic tests, the wall was pushed further into the backfill in order to mobilize a significant portion (268 kN/m) of the expected peak passive resistance (Figure 4). Input excitations of 100%, 200%, and 300% (1x, 2x, and 3x) of the STM were imparted by the shake table with the wall locked in this near passive pressure condition. For this test series, Figures 13-15 show the total force measured by the load cells, normalized per meter of wall length, and the ground surface acceleration (near the wall). The relationship between force and acceleration is shown in

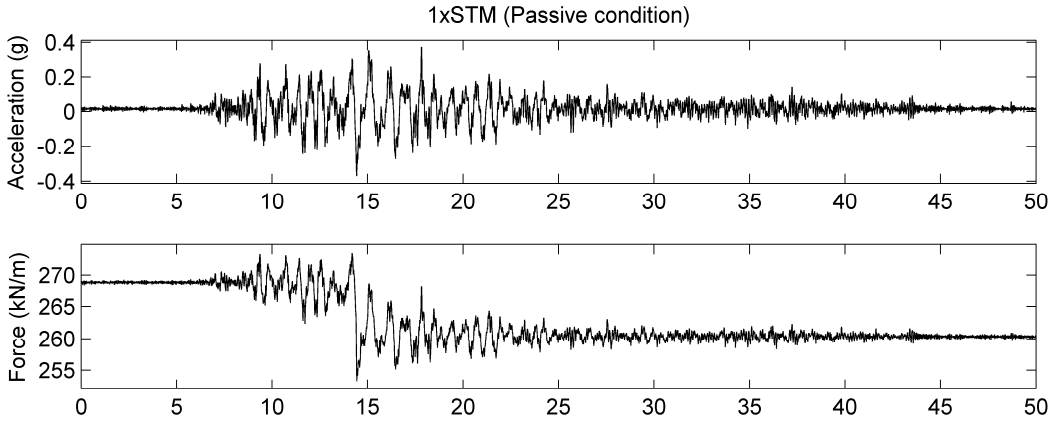

Figure 13: ***Backfill acceleration and total load cell force for the baseline STM (near passive condition).***

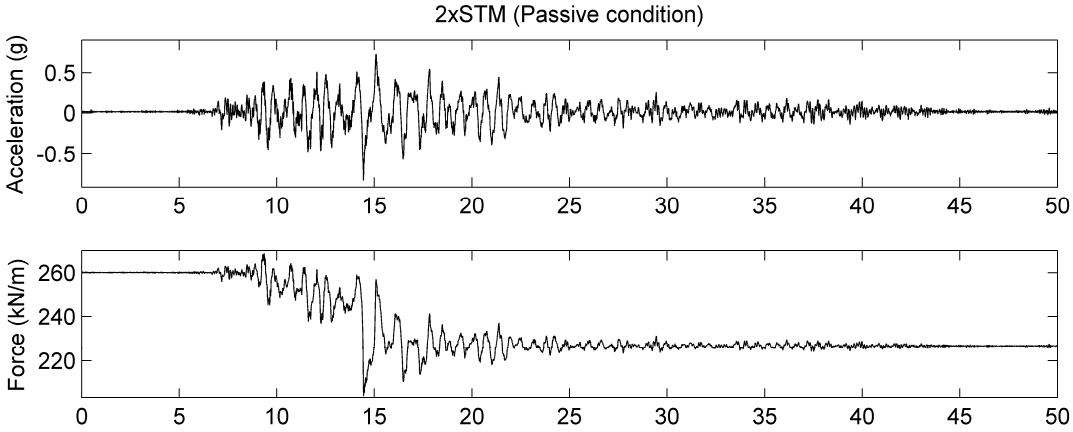

Figure 14: ***Backfill acceleration and total load cell force for 2 x STM (near passive condition).***

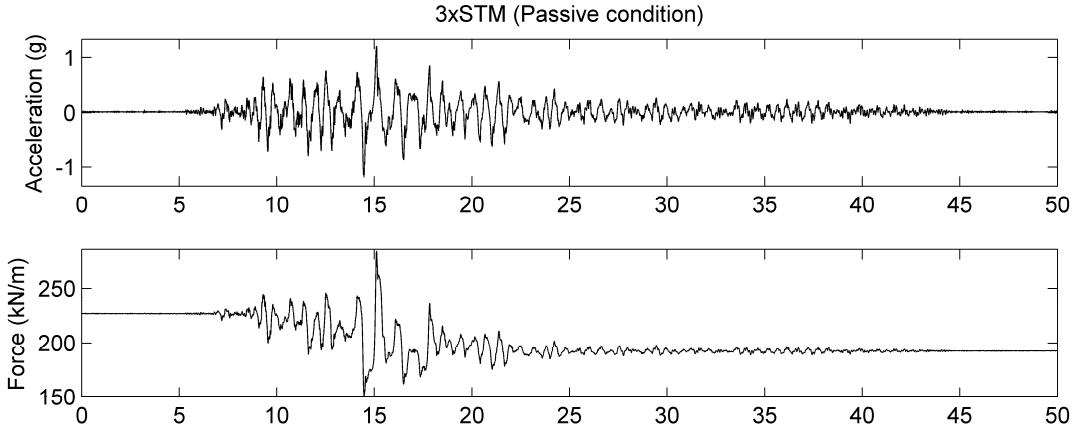

Figure 15: ***Backfill acceleration and total load cell force for 3 x STM (near passive condition).***

Figure 16. Earth pressure thrust variation with acceleration is depicted in Figure 17, where the wall inertial force has been removed as discussed earlier.

Noting that the above experiments were conducted in sequence (starting with the 1x STM shaking event), passive thrust at the beginning of the shaking events (1x, 2x, and 3x STM) was respectively reduced by (Figures 13-15): i) as much as 6%, 21%, and 33% during the shaking phase, and ii) 3%, 13%, and 15% at the end shaking. Such a variation in pressure could substantially affect the instantaneous available resistance against potential bridge-deck displacement during a seismic event.

Analysis of the Experimental Observations

The near passive condition dynamic response bears some similarities to that of the earlier near at-rest case (Figures 6 through 9). Minor changes in thrust continue to prevail within the 0.5g range of acceleration (Figures 16 and 17). At higher g-levels, the force acting on the wall starts to significantly increase (Figures 15, 16c and 17c).

However, some notable differences may be seen in Figures 13 through 17 compared to the earlier near at-rest response (Figures 6 through 9). For instance, a major reduction in the static thrust component is observed in the passive case (Figures 13 through 15). During the strong shaking phase, this static component of passive pressure is seen to undergo phases of gradual decrease. The initial high lateral stresses

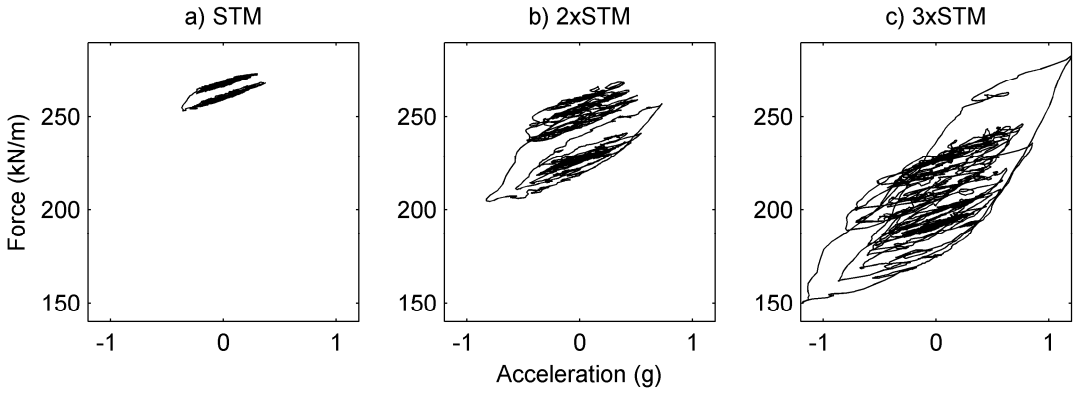

Figure 16: ***Total load cell force versus backfill acceleration (near passive condition).***

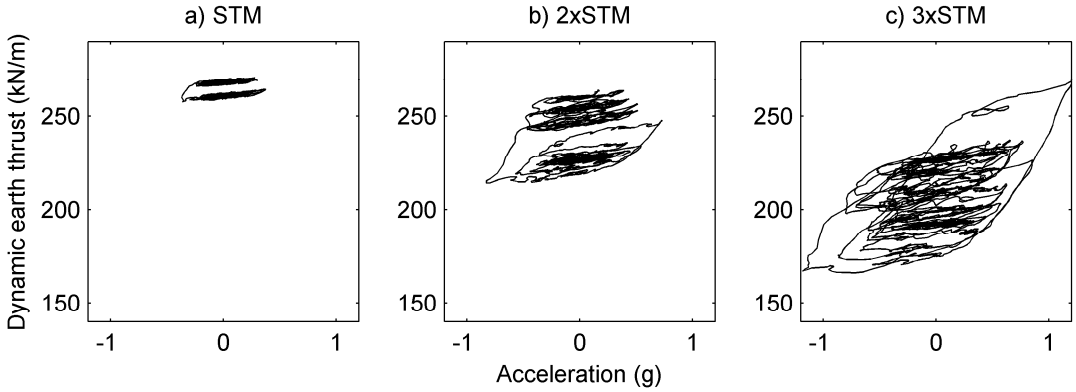

Figure 17: ***Dynamic earth thrust versus backfill acceleration (near passive condition).***

become partially relieved as the system is shaken, allowing a tendency for the soil to heave upwards in the direction of the lower static principal stress. As a consequence, lateral stresses are relieved incrementally during the cycles of large amplitude acceleration.

SUMMARY AND CONCLUSIONS

A full-scale shake table test configuration was constructed to measure lateral earth pressure under static (passive) and dynamic loading scenarios. Recorded static passive earth resistance was presented in the form of a force-displacement backbone curve. The measured dynamic thrust for both the at-rest and passive pressure conditions was shown in the form of force-time histories and force-acceleration relationships. Conclusions based on the test results include [2]:

1. The static passive resistance provided by the dense sand backfill increased with displacement reaching a peak value (close to Log-Spiral prediction), and decreased thereafter to a lower residual level. Design load-deflection models [11, 12] agree with the experimentally measured data up to the peak resistance, but do not represent the softening behavior that was observed at large deflections (greater than about 5 cm). This issue may warrant further investigation.

2. At dynamic excitations of up to about 0.5g, changes in the lateral force measured behind the wall (on the bridge side) may be due primarily to its inertia. Up to this level, the dynamic earth pressure increment was quite low for the tested soil backfill. Cohesion in this sandy soil (c of about 14 kN/m^2) is thought to contribute to this minimal variation in dynamic earth pressure at such shaking levels.

3. At larger dynamic excitations (above about 0.5g), the measured dynamic lateral forces began to increase at a relatively high rate. In addition to the wall inertial force, dynamic earth pressure played a progressively dominant role with the increase in lateral acceleration.

4. At the instants of large acceleration, available passive earth resistance to bridge deck displacement may substantially depend on the magnitude and direction of the excitation. In the experimental results, compared to the static value, a possible change of about 30% was observed at a 1g level of peak acceleration. Therefore, the actual resistance provided by the abutment may fall within a significant range of the measured static force-displacement relationship. This consideration strongly motivates future combined bridge-backfill interaction shake-table testing, in order to further quantify this mechanism.

5. A portion of the mobilized static passive stress within the backfill was relieved during the strong shaking phase. After the shaking event, the static lateral load decreased by as much as 15%. Implications of this mechanism would be also further quantified through shake table experimentation of the combined bridge-abutment configuration.

6. Figures 13 through 16 in addition to the backbone curve of Figure 4 constitute a set of data that provides a basis for calibration of nonlinear finite element (FE) models. Such abutment-backfill models would account for the static passive force-displacement capacity and the dynamic pressure contributions (Figure 1) in numerical bridge model simulations.

ACKNOWLEDGMENTS

Funding for this research was provided by the National Science Foundation (NSF) NEES-R grant number 0420347 under the overall direction of Professor M. Saiid Saiidi of the University of Nevada at Reno (UNR). In addition, support was provided via the UCSD Englekirk Fellowship. The authors are grateful to Dr. Anoosh Shamsabadi of Caltrans for providing valuable advice and insight regarding the employed testing configuration. Use of geotechnical testing facilities and services provided by Mr. Joseph Vettel of Geocon Consultants, Inc. (San Diego, California) contributed

to the success of this research program. Professor Scott Ashford kindly allowed for use of the employed soil container.

REFERENCES

1 Saiidi, M.S. (2004). "Seismic Performance of Bridge Systems with Conventional and Innovative Design." <http://nees.unr.edu/4-spanbridges/index.html>

2 Wilson, P. (2009). "Full-scale modeling and simulation of lateral earth pressure for bridge abutment seismic design." Ph.D. thesis, Dept. of Structural Eng., Univ. of California, San Diego, CA (In progress).

3 Shamsabadi, A., Ashour, M. and Norris, G. (2005). "Bridge abutment nonlinear force-displacement-capacity prediction for seismic design," *Journal of Geotechnical and Geoenvironmental Engineering*, ASCE, **131**(2): 151-161.

4 Cole, R., and Rollins, K. (2006). "Passive earth pressure mobilization during cyclic loading." *Journal of Geotechnical and Geoenvironmental Engineering*, ASCE, **132**(9): 1154-1164.

5 Bozorgzadeh, A. (2007). "Effect of structure backfill on stiffness and capacity of bridge abutments." Ph.D. thesis, Dept. of Structural Eng., Univ. of California, San Diego, CA.

6 Stewart, J. P., Taciroglu, E., Wallace, J, W., Ahlberg, E. R., Lemnitzer, A., Rha, C., Tehrani, P. K., Keowan, S., Nigbor, R. L., and Salamanca, A. (2007). *Full scale cyclic testing of foundation support systems for highway bridges. Part II: Abutment backwalls*, UCLA – SGEL, Report 2007/02, Department of Civil Engineering, Univ. of California, Los Angeles, CA.

7 Shirato, M., Fukui, J., and Koseki, J. (2006). "Current status of ductility design of abutment foundations against large earthquakes," *Soils and Foundations*, Japanese Geotechnical Society, **46**(3): 377-396.

8 Koseki, J., Tatsuoka, F., Munaf, Y., Tateyama, M. and Kojima, K., (1998). "A modified procedure to evaluate active earth pressure at high seismic loads," *Special Issue of Soils and Foundations*, Japanese Geotechnical Society: 209-216.

9 Koseki, J., Watanabe, K., Tateyama, M. and Kojima, K. (2001). "Seismic earth pressures acting on reinforced and conventional type retaining walls," *Landmarks in Earth Reinforcement*, Ochiai et al. (eds), Swets & Zeitlinger, Lisse, The Netherlands: 393-398.

10 Applied Technology Council and the Multidisciplinary Center for Earthquake Engineering Research (ATC/MCEER) (2001). Recommended LRFD guidelines for the seismic design of highway bridges: 8-14 to 8-17.

11 Caltrans (2004). Seismic design criteria. California Department of Transportation, Sacramento, CA: 7-28 to 7-31.

12 AASHTO (2007). Proposed Guide Specifications for LRFD Seismic Bridge Design. American Association of State Highway and Transportation Officials, Washington D.C.

13 Maroney, B. H. (1995). "Large-scale abutment tests to determine stiffness and ultimate shear strength under seismic loading." Ph.D. thesis, Univ. of California, Davis, CA.

14 Mononobe, N. and Matsuo, H. (1929). "On the determination of earth pressures during earthquakes," *Proceedings, World Engineering Congress*

15 Okabe, S. (1926). "General theory of earth pressures," *Journal of the Japan Society of Civil Engineering*, **12**(4): 34-41.

16 Kramer, S. (1996). *Geotechnical Earthquake Engineering*. Prentice Hall, Upper Saddle New Jersey.

17 UCSD (2003). "Englekirk Center, Powell Structural Laboratories," http://www.jacobsschool.ucsd.edu/Englekirk/

18 Restrepo, J. I., Conte, J. P., Luco, J. E., Seible, F., Van Den Einde, L. (2005), "The NEES@UCSD Large High Performance Outdoor Shake Table Earthquake Engineering and Soil Dynamics (GSP 133)", *Proc. Geo-Frontiers 2005, Sessions of the Geo-Frontiers 2005 Congress*, R. W. Boulanger, M. Dewoolker, N. Gucunski, C. H. Juang, M. E. Kalinski, S. L. Kramer, M. Manzari, and J. Pauschke, Eds, January 24–26, Austin, Texas, USA.

19 Caltrans (1999). "Standard specifications." California Dept. of Transportation, Sacramento, CA.

20 Duncan, M., and Mokwa, R. (2001). "Passive earth pressures: theories and tests," *Journal of Geotechnical and Geoenvironmental Engineering*, ASCE, **127**(3): 248-257.

21 Terzaghi, K., Peck, R., and Mesri, G. (1996). Soil *mechanics in engineering practice, 3rd edition*, John Wiley and Sons, Inc. New York, NY.

22 Lambe, T. W. and Whitman, R. V. (1969). *Soil mechanics*. John Wiley & Sons, Inc., New York, NY.

23 Wood, J. (1973). "Earthquake-induced soil pressure on structures," *Report EERL 73-05*, California Institute of Technology, Pasadena, California.

24 Rao, K. S. and Choudhury, D. (2005). "Seismic passive earth pressures in soils," *Journal of Geotechnical and Geoenvironmental Engineering*, ASCE, **131**(1): 131-135.

25 Mylonakis, G., Kloukinas, P., Papantonopoulos, C., (2007). "An alternative to the Mononobe-Okabe equations for seismic earth pressures," *Soil Dynamics and Earthquake Engineering*, Elsevier **27**: 957-969.

26 Wu, G. and Finn, W. D. (1999). "Seismic lateral pressures for design of rigid walls," *Canadian Geotechnical Journal*, NRC, Vol. 36: 509-522.

27 Nakamura, S. (2006). "Reexaminations of Mononobe-Okabe theory of gravity retaining walls using centrifuge model tests," *Soils and Foundations*, Japanese Geotechnical Society, **46**(2): 135-146.

28 Sitar, N., and Al Atik, L. (2008). "Dynamic centrifuge study of seismically induced lateral earth pressures on retaining structures," Zeng, D., Manzari, M., and Hiltunen, D., Eds., *Proceedings, Geotechnical Earthquake Engineering and Soil Dynamics IV*, ASCE., Sacramento, CA.

29 Anderson, D. G., Martin, G. R., Lam, I. P., and Wang, J. N. (2008). "Proposed changes to AASHTO LRFD bridge design specifications for the seismic design of retaining walls," Zeng, D., Manzari, M., and Hiltunen, D., Eds., *Proceedings, Geotechnical Earthquake Engineering and Soil Dynamics IV*, ASCE., Sacramento, CA.